Experimental Results of Sub-Y-Type Array for High Angular Resolution Interferometric Radiometer at 37 GHz

Gumsil Kang, Sunghyun Kim, Junho Choi, and Yonghoon Kim
Department of Mechatronics, Kwangju Institute of Science and Technology,
1 Oryong-dong, Buk-gu, Gwangju 500-712, Korea
kgs@kjist.ac.kr

Abstract: The Sub-Y-type array is proposed to decrease the number of antennas keeping same resolution or to use same number of antennas in order to have a narrow 3dB beamwidth. When the sub-Y-type array is designed with 136 antennas for comparison with MIRAS, the reduction rate is theoretically 30 %. The proposed ideas are evaluated by experimental interferometric radiometer at 37 GHz.
Keywords: Interferometric synthetic aperture radiometer, sub-Y-type.

1. Introduction

The 2-D interferometric synthetic aperture radiometer (ISARad) has been developed to obtain a high angular resolution image for the earth remote sensing [1]-[3]. The ISARad measures indirectly the brightness temperature image of object from the visibility function sampled by 2-D static array of small antennas without scanning [1]-[3]. It has been reported that Y-type array with equally spaced antennas are optimal in terms of a narrow beamwidth and wide synthesized FOV. For such as MIRAS (Microwave Imaging Radiometer by Aperture Synthesis), large Y-type array with 43 antennas per arm spaced 0.89 λ at 1.4 GHz is used in order to obtain 3 dB beamwidth of 0.77° [4], [5]. The requirement for large array to get a high spatial resolution is one of the controversial points, because it causes problems such as complexity and system cost which are obstacles for the commercial application of ISARad as passive imager. This study suggests the sub-Y-type array to decrease the number of antennas keeping same resolution in comparison with Y-type array.

The relationship between visibility function and reconstructed image is briefly introduced to explain the proposed idea. Fig. 1 shows the geometry of interferometric measurement for aperture synthesis. The output of the complex cross correlator is called the visibility function. If all antennas, amplifiers, filters and correlators are identical and ideal, and the baseband brightness process has suffered little decorrelation between two antennas, then the brightness temperature image can be indirectly generated by the following discrete 2-D IFFT

$$\hat{T}_B(\zeta,\eta) = \sum_u \sum_v W(u,v)\, V(u,v) \exp[\, j2\pi(u\zeta + v\eta)] \tag{1}$$

where $u = D_x/\lambda$, $v = D_y/\lambda$, $\zeta = \sin\theta\cos\phi$, $\eta = \sin\theta\sin\phi$ and $W(u,v)$ represents a weight function used to decrease the sidelobe level. Since the shape of array decides the sampling characteristic of visibility function, the imaging characteristics depend on the array shape. The synthesized 3 dB beamwidth of array becomes narrow proportionally to the sample coverage of visibility function.

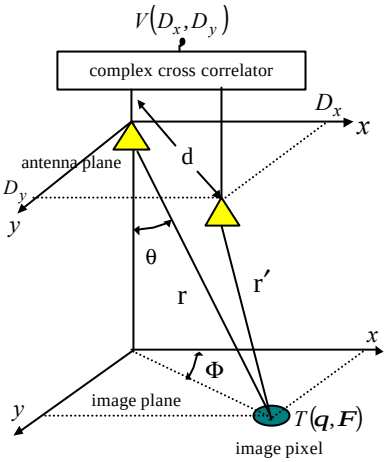

Fig. 1. Interferometric measurement geometry.

2. Sub-Y-type Array

The sub-Y-type array shown in Fig. 2 is designed to obtain wide visibility coverage at the expense of incomplete sampling. It is based on antenna groups, which consist of two sub-arrays spaced by d_2. The sub-array is Y-type array with four antennas arranged by d_1.

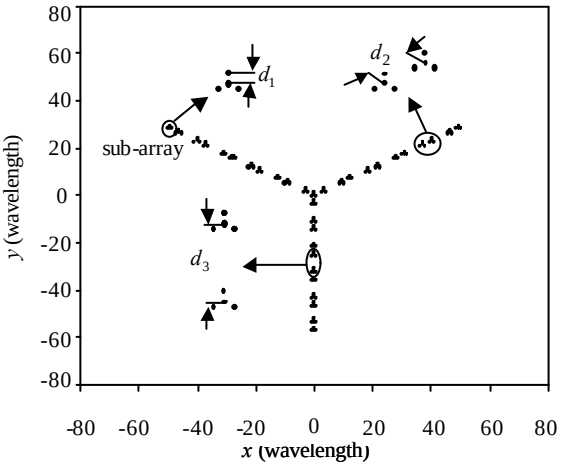

Fig. 2. Sub-Y-type array with 136 antennas.

The distance d_2 is set to $4d_1$ to obtain a complete sampling on the principle axes, which is required for alias suppression algorithm described in next section. The grouping of sub-arrays in Fig.2 is intended to extent the arm of sub-Y-type array keeping a complete sampling on the principle axes. The spacing between two groups is represented by d_3. For comparison with MIRAS, the array shown in Fig. 2 is designed using a total number of 136 antennas. The antenna spacing of MIRAS, 0.89λ, is chosen for d_1.

Sampling characteristic of visibility coverage for sub-Y-type array is different from that of the Y-type array. The coverage area includes the blank areas, where samples of visibility function are missed, except on the principle axis, while the Y-type array provides a complete sampling. These blank areas cause alias effect. However, the alias effect can be reduced by –15 dB with a rectangular window by alias suppression method suggested in [6].

3. Effects of d_3 on the Angular Resolution and the Alias Suppression

For sub-Y-type array shown in Fig. 2, the 3dB beamwidth and alias effect are a function of the spacing d_3 because the area of visibility coverage and the blank area depend on the spacing d_3 [6]. When the spacing d_3 is extended, the 3 dB beamwidth is reduced, while the aliasing level is increased because the non-sampled region becomes wider as well as the visibility coverage. However the alias effect can be suppressed by alias suppression algorithm based on 1-D alias-free profile. But if the spacing d_3 is too extended to obtain the alias-free profile at $u = 0$, $v = 0$, the performance of alias suppression is degraded. Fig. 3 shows beamwidth reduction rate and main beam efficiency of alias-suppressed point source response according to d_3 when the number of antennas equals to 136. The reduction rate R is computed from 3 dB width of sub-Y-type array and Y-type by

$$R = \frac{\theta_Y - \theta_{Sub-Y}}{\theta_Y} \times 100 \ (\%) \qquad (2)$$

where θ_Y^C and θ_{Sub-Y} are the 3 dB beamwidth of the Y-type and the sub- Y-type, respectively. The Y-type array with equally spaced antennas by d_1 is assumed as like MIRAS. The main beam efficiency η_m of point source response is computed according to the equation [2]

$$\eta_m = \frac{\iint_{main\,\mathrm{lobe}} |P(\theta,\phi)| \sin\theta \, d\theta \, d\phi}{\iint_{4\pi} |P(\theta,\phi)| \sin\theta \, d\theta \, d\phi} \qquad (3)$$

where $P(\theta,\phi)$ means the point source response.

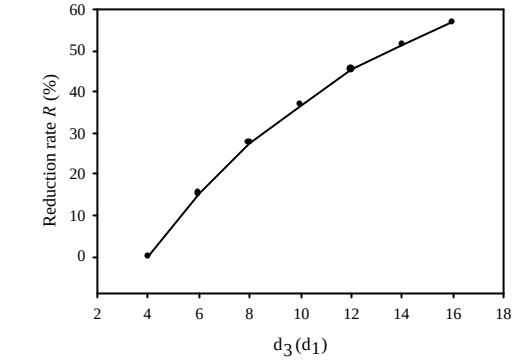

(a)

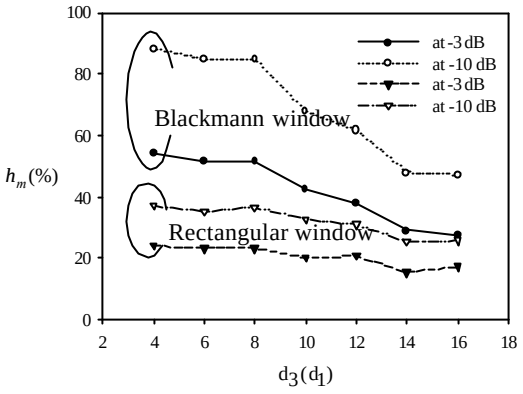

(b)

Fig. 3. Effect of d_3 on the alias-suppressed image of point source. (a) Reduction rate of 3dB beamwidth, (b) Main beam efficiency of point source response η.

When d_3 equals to $4d_1$, the 3 dB beamwidth of sub-Y-type and Y-type are same. The reduction rate R increases according to d_3 in Fig. 3(a). The main beam efficiency η is calculated to estimate the alias suppression. For sub-Y-type array shown in Fig. 2, $8d_1$ is maximum extension for d_3 to achieve the alias-free profiles at $u = 0$, $v = 0$. At this point η begins to decrease in Fig. 3(b), and the reduction rate of 3 dB beamwidth is about 30 %. When the spacing d_3 is fixed, the reduction rate of sub-Y-type depends on the number of antennas. Fig. 4 shows the reduction rate as a function of number of antennas when the spacing d_3 equals to $8d_1$.

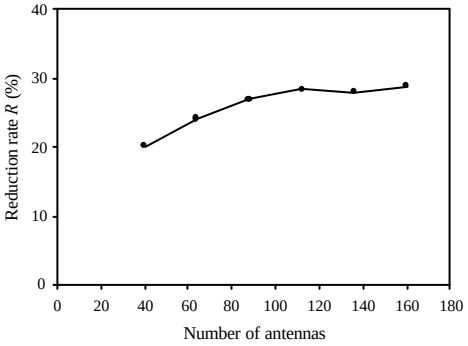

Fig. 4. Reduction rate according to the number of antennas.

4. Experimental Results

For the experiment, the 37 GHz correlation radiometer is developed and the major experimental parameters are summarized in Table 1. The sub-Y-type array is designed with 40 antennas instead of 136 to avoid experimental complexity. The $8d_1$ is chosen for spacing d_3 of sub-Y-type to obtain the good alias suppression as well as high angular resolution. For this sub-Y-type array, the measurement range between noise point source and radiometer should be longer than 14.7 m to meet far-field condition. But in fact receiving antennas are 4m from noise source because of the limitation of our experimental setup. Therefore the phase error due to the spherical wave front is caused. In order to keep the same phase error for Y-type and sub-Y-type, the Y-type is constructed with 52 antennas for experiment so that the same visibility coverage of sub-Y-type with 40 antennas is achieved. Fig. 5 shows the experimental setup.

Fig. 5. Experimental radiometer at 37 GHz.

Table1. Measurement Parameters.

Centre frequency	37 GHz
Correlation bandwidth	100 MHz
Integration time	0.65 μs
Measurement range	4 m

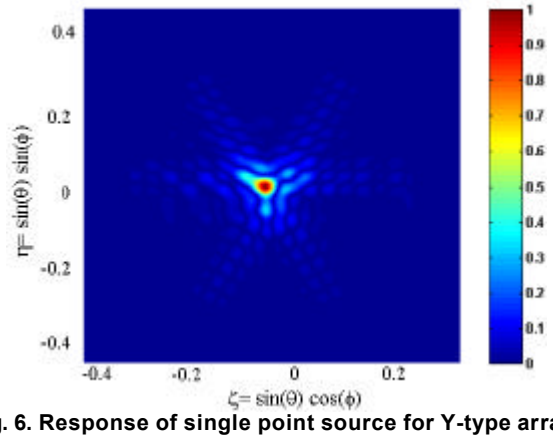

Fig. 6. Response of single point source for Y-type array.

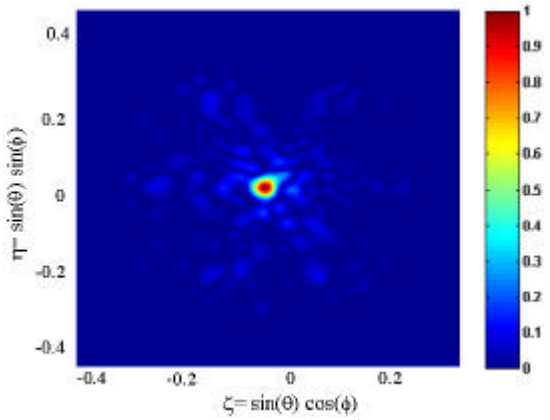

Fig. 7. Alias suppressed response of single point source.

5. Conclusions

The imaging characteristics of sub-Y-type array are analyzed not only theoretically, but also experimentally. It is observed that the main beam efficiency η_m begins to decline when the d_3 equals to $8d_1$. Under this condition, 30 % reduction rate R is achieved. Experimental results indicate that the number of antennas required for obtaining the 3 dB beamwidth 2.5° is reduced by 23% in comparison with Y-type.

Acknowledgement

This work was supported in part by the Korean Science and Engineering Foundation (KOSEF) through the Advanced Environmental Monitoring Research Center at Kwangju Institute of Science and Technology.

References

[1] G. W. Swenson, JR., and N. C. Mathur, 1968. The Interferometer in Radio Astronomy, *Proceedings of the IEEE*, vol. 56, no. 12, pp. 2114-2129.

[2] C. S. Ruf, C. T. Swift, and A. B. Tanner, 1988. Interferometric Synthetic Aperture Microwave Radiometry for the Remote Sensing of the Earth, " *IEEE Transactions on Geo. and Remote Sensing*, vol. 26, no. 5, pp. 597-611.

[3] A. Camps, F. Toress, I. Corbella, J. Bara, and X. Soler, 1997. Calibration and Experimental Results of a Two-Dimensional Interferometric Radiometer Laboratory Prototype, *Radio Science*, vol. 32, no. 5, pp. 1821-1832.

[4] A. Camps, J. Bara, I. Corbella, and F. Toress, 1997. The Processing of Hexagonally Sampled Signals with Standard Rectangular Techniques: Application to 2-D Large Aperture Synthesis Interferometric Radiometers, *IEEE Transactions on Geoscience and Remote Sensing*, vol. 35, no. 1, pp. 183-190, 1997.

[5] J. Bara, A. Camps, F. Toress, and I. Corbella, 1998. Angular Resolution of Two-Dimensional, Hexagonally Sampled Interferometric Radiometers, *Radio Science*, vol. 33, no. 5, pp. 1459-1473, 1998.

[6] Gumsil Kang and Jing-Shan Jiang, 2002. Sub-Y-Type Antenna Array Configuration for High Resolution Interferometric Synthetic Aperture Radiometer, *Proceeding of ISRS 2002* pp. 581-586,Oct.30-Nov.1.